Resonant inelastic soft x-ray scattering and electronic structure of LiBC

2004 J. Phys.: Condens. Matter 16 5137

(http://iopscience.iop.org/0953-8984/16/28/031)

INSTITUTE OF PHYSICS PUBLISHING JOURNAL OF PHYSICS: CONDENSED MATTER

J. Phys.: Condens. Matter **16** (2004) 5137–5142 PII: S0953-8984(04)74703-7

Resonant inelastic soft x-ray scattering and electronic structure of LiBC

P F Karimov[1], N A Skorikov[1], E Z Kurmaev[1], L D Finkelstein[1], S Leitch[2], J MacNaughton[2], A Moewes[2] and T Mori[3]

[1] Institute of Metal Physics, Russian Academy of Sciences Ural Division, 620219 Yekaterinburg GSP-170, Russia
[2] Department of Physics and Engineering Physics, University of Saskatchewan, 116 Science Place, Saskatoon, Saskatchewan S7N 5E2, Canada
[3] National Institute for Materials Science, Advanced Materials Laboratory Namiki 1-1, Tsukuba 305-0044, Japan

Received 13 January 2004
Published 2 July 2004
Online at stacks.iop.org/JPhysCM/16/5137
doi:10.1088/0953-8984/16/28/031

Abstract

The electronic structure of LiBC has been studied using soft x-ray fluorescence measurements. Resonant inelastic x-ray scattering (RIXS) spectra were measured with the excitation energy tuned to the boron and carbon K-edges. RIXS spectra show dispersive features, which were assigned to the calculated energy bands using the site-selective quantitative band mapping method based on the concept of k-momentum conservation. It is concluded that while the electronic structure calculations are in general agreement with experimental spectra, carbon and boron K-emission bands show some deviation due to an incomplete hybridization of the C 2p–B 2p states.

1. Introduction

The discovery of superconductivity in MgB_2 ($T_c = 39$ K) [1] has stimulated strong interest in related layered compounds. The crystal structure of MgB_2 is similar to intercalated graphite [2], with the boron atoms replacing carbon. LiBC is a large gap semiconductor [3] that has a comparable crystal structure to MgB_2, with boron and carbon atoms alternately occupying the sites within the hexagonal sheets. Since σ holes contribute to superconductivity in MgB_2 [4], attempts have been made to achieve the same result by doping LiBC. Band structure calculations involving supercells of Li_xBC for $x = 1.0$, 0.75, and 0.5 [5] show that the Fermi level moves into the valence band as x decreases. This behaviour near the Fermi level is similar to that of the rigid band model. These idealized model calculations for ordered Li-deficient compounds predict that introducing off-stoichiometric Li could give rise to a finite density of states at the Fermi level and make the system metallic [5–8]. The Li-deficient compound has been suggested to be superconducting with T_c as high as 100 K [5]. Specifically, 65 K has been predicted for an Li stoichiometry of 0.5 [7].

Following these theoretical predictions, several attempts to synthesize Li-deficient Li_xBC have been made to establish superconductivity in this system [9, 10]. So far no characteristics associated with a superconducting transition, such as a diamagnetic signal or zero resistance, have been observed in Li-deficient LiBC at low temperatures.

To understand why predictions of high-T_c superconductivity based on band structure calculations have failed, the calculated energy bands of LiBC must be compared to experimental spectra. The electronic structure calculations of Li-deficient LiBC are derived from those of the stoichiometric compound using the rigid band model. Therefore, it is useful to check the validity of the band structure calculations of stoichiometric LiBC. Then the correctness of this model for simulation of off-stoichiometric LiBC can be determined. To analyse these questions we present the first experimental RIXS study of LiBC and compare the results with our linear muffin-tin orbitals (LMTO) band structure calculations.

2. Experimental and calculation details

In the synthesis of LiBC, crushed Li metal chunks (99.9%), amorphous boron powder (99.9%), and graphite (99.9%) were mixed inside an He glovebox. The mixture was sealed in Ta cells and inductively heated in a BN crucible surrounded by a graphite susceptor to 940–1020 °C for 10–14 h. The resulting LiBC powder was pressed into pellets at 3000 atm and annealed. The samples were structurally characterized using high-resolution powder x-ray diffractometry with Cu Kα-radiation.

Measurements of stoichiometric LiBC were performed at the soft x-ray fluorescence endstation located at Beamline 8.0 of the Advanced Light Source at the Lawrence Berkeley National Laboratory. The emitted radiation is partially collected in a Rowland circle-type spectrometer with spherical gratings and recorded by an area sensitive multi-channel detector. This combination provides an instrumental resolution of about 0.4 eV at the C and B Kα emission energies. The x-ray absorption spectra were measured in partial fluorescence and total electron yield (PFY and TEY) mode. The resolving power $E/\Delta E$ for the absorption spectra was 5000. Additional spectral broadening occurs due to the core hole lifetime. For boron and carbon K-edge spectra, the core level width is approximately 0.2–0.3 eV. All absorption and emission spectra are normalized to the number of photons falling on the sample, monitored by a gold mesh in front of the sample.

The available band structure calculations for LiBC [5, 6] are limited because they consist of only the total density of states, and the $E(k)$-curves are calculated for an energy range insufficient for understanding the RIXS spectra. This was the motivation for our calculation of total and partial DOS and $E(k)$ dispersion curves for LiBC for the extended energy region of -15 to +20 eV. We calculated the electronic structure of LiBC using a self-consistent linearized muffin-tin orbital (LMTO) method (TBLMTO-47 computer code [11]). The von Barth–Hedin parametrization is used for the exchange correlation potential within the local density approximation. Brillouin zone (BZ) **k**-point integrations were made using the tetrahedron method on a grid of 549 k-points in the irreducible part of the BZ. The crystal structure of LiBC was modelled by the space group $P6_3/mmc$, D^4_{6h}, No. 194, and the lattice parameters were $a = 2.752$ Å, $c = 7.058$ Å $= 2 \times 3.529$ Å with coordinates of the atoms Li (2a) (0 0 0), B (2c) (1/3 2/3 1/4) and C (2d) (1/3 2/3 3/4) [3]. The B and C atoms form a planar heterographite layer with a B–C distance of 1.589 Å and the Li atoms fill the interlayer regions. The unit cell along the hexagonal axis is doubled due to the interchange of boron and carbon positions in neighbouring planes [3].

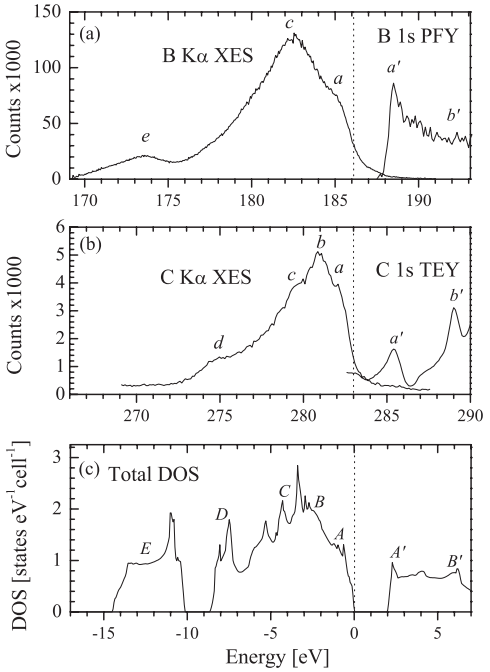

Figure 1. Comparison of (a) boron absorption spectrum and K-emission spectrum at 210.0 eV and (b) carbon absorption spectrum and K-emission spectrum at 310.0 eV with (c) calculated total density of states of LiBC.

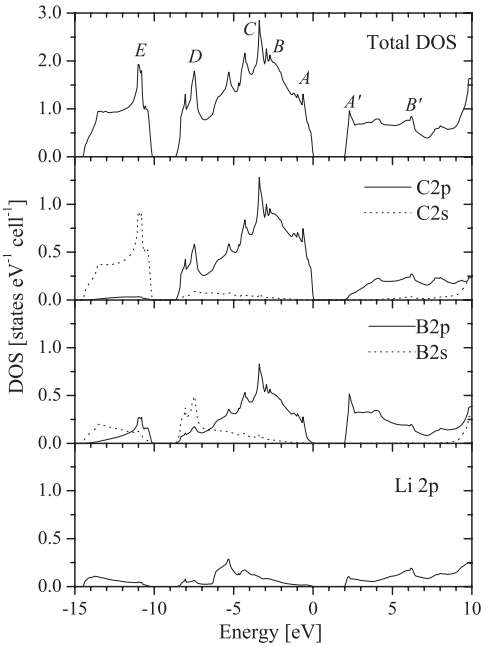

Figure 2. Calculated total and partial DOS of LiBC.

3. Results and discussion

The measurements of non-resonant (excited well above threshold) carbon and boron Kα x-ray emission spectra (XES) and the C 1s and B 1s x-ray absorption spectra (XAS) of LiBC are presented in figures 1(a) and (b). Taking into account the dipole selection rules, these element-specific spectra probe the local occupied and unoccupied states of p symmetry. Figure 1(c) displays the calculated total density of states of LiBC with the energy axis adjusted to correspond to experimental data for comparison.

In our calculations (figure 2) the carbon and boron 2p states mainly contribute to the density of states at the top of the valence band, near the Fermi level, whereas Li provides very little contribution to the total DOS at this energy. The features labelled a in the carbon and boron K-emission bands in figure 1 and the feature labelled A of the total DOS indicate that the valence band state density is a direct result of the contributions from the boron and carbon occupied states. The additional emission features b and c as well as the main absorption features a′ and b′ of the B 1s TFY and C 1s TEY spectra can be related to the main subbands B and C along with A′ and B′ in the total DOS. Spectral feature d in the carbon K-emission band corresponds to the calculated subband D, resulting from a B 2s–C 2p hybridization (see figure 2). Likewise, feature e in the boron XES spectrum in figure 1 aligns with the calculated E subband, resulting from C 2s–B 2p hybridized states.

The band structure calculations show similar contributions from both C 2p and B 2p states for features A, B and C. However, experimental carbon and boron K-emission spectra do not

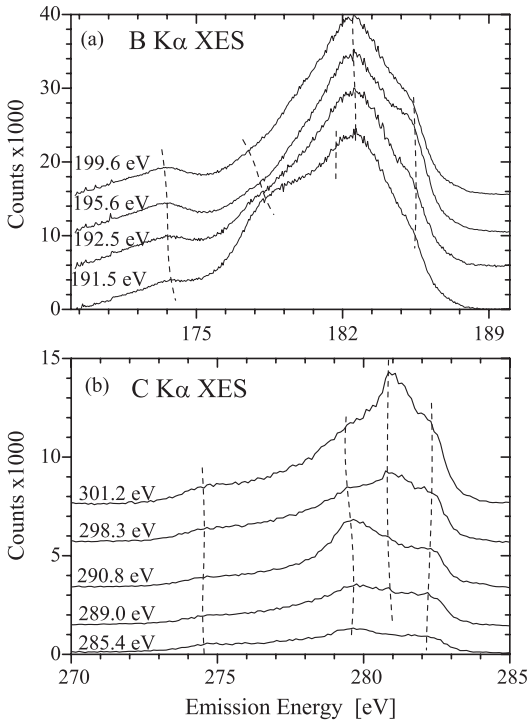

Figure 3. Resonant boron (a) and carbon (b) K-emission bands of LiBC. Excitation energies are displayed at the left of the spectra.

indicate the same contributions. Features a, b and c appear in C Kα emission, while in B Kα emission, only features a and c appear. This means that in spite of C 2p–B 2p hybridization carbon and boron 2p-states keep their individual character due to their chemical difference.

The results of our calculations of stoichiometric LiBC are in agreement with previous calculations [5, 6]. The calculated DOS predicts a value for the insulating gap between the π^* conduction band and the π valence band of approximately 2 eV. This is an underestimate, a well-known characteristic of LDA calculations. Likewise, it is rather difficult to estimate the band gap from the experimental spectra because of smearing effects due to the core hole lifetime and instrumental distortion, as well as the existence of impurity states.

Resonant boron and carbon Kα XES of LiBC displayed in figure 3 are strongly dispersive. Therefore, LiBC is a promising candidate for RIXS band mapping [12]. The interpretation of RIXS spectra is based on the concept that x-ray absorption and emission events should be treated as a single inelastic scattering process with conserved crystal momentum [13]. When a core electron is promoted to the conduction band, an emission occurs from the valence band with the same **k**-value. Crystal momentum is determined by the selection of excitation energy.

RIXS can be used for insulators and polycrystalline materials (such as LiBC), which are difficult or impossible to study by the alternative angle-resolved ultraviolet photoemission (ARPES). A disadvantage of RIXS is that the **k**-selectivity is given indirectly and depends on the dispersion of the unoccupied bands. Only at special points, such as band edges and high symmetry points, can **k** be determined unambiguously from inelastic scattering experiments.

We performed quantitative band mapping for LiBC using experimental RIXS data. Features of the boron and carbon emission spectra were extracted from the comparison to the first and second derivatives and are labelled using dashed lines in figure 3. An example of this method to determine features is displayed in figure 4. The dotted horizontal lines in

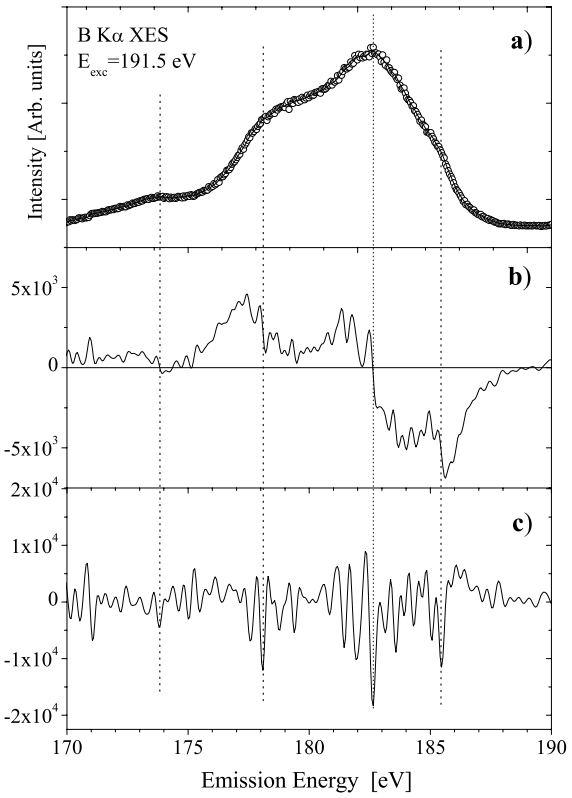

Figure 4. Comparison of B Kα XES of (a) LiBC measured at $E_{\mathrm{exc}} = 191.5$ eV (circles) and FFT smoothing (line) of the curve to (b) the first derivative and (c) second derivative demonstrates the method of determining spectral features.

figures 5(a) and (b) correspond to the excitation energies selected for the RIXS at the B and C K-edges. The electrons are excited to states where these lines intersect with dispersion curves for the unoccupied states indicating possible **k**-values. Since **k**-momentum is conserved, the inelastic emission results from points where a vertical line from each excited state intersects with the occupied states. The points derived from these procedures are labelled by symbols in figure 5, where each symbol corresponds to a particular excitation energy. The experimental points are generally found to be close to the calculated energy bands in the region of occupied electronic states, demonstrating a general agreement between experiment and theory.

4. Conclusion

To summarize, the comparison of experimental RIXS data with our density functional theory calculations shows that in spite of a general agreement between experimental and calculated energy bands of stoichiometric LiBC, carbon and boron electronic states do not completely hybridize, retaining some of their individual character. With this in mind, the lack of superconductivity in off-stoichiometric LiBC could be due to several different reasons:

(1) the lack of complete hybridization of the B and C states, which is inconsistent with the calculations;
(2) high chemical stability of LiBC reduces hole doping due to Li-deintercalation; and
(3) preparational factors such as a B–C disorder [8] or a strong structural relaxation in the vicinity of the hole dopants [9] are known to be crucial for superconductivity and are not currently taken into account in the LDA model calculations of hole-doped LiBC.

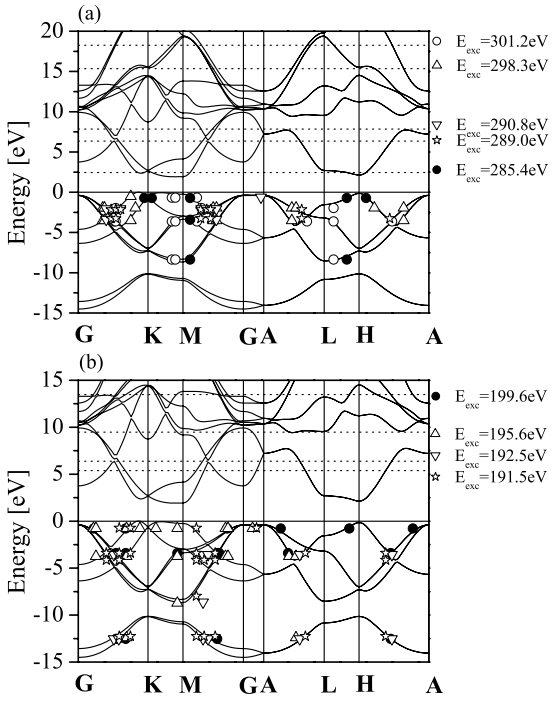

Figure 5. Band mapping of LiBC using RIXS measured at (a) carbon and (b) boron K-edges; the curves show the calculated band structures and the symbols represent the experimental results for various excitation energies. Zero on the calculated energy scales corresponds to carbon emission energy of 283.0 eV in (a) and boron emission energy of 186.1 eV in (b).

Acknowledgments

Funding by the Research Council of the President of Russian Federation (Project NSH-1026.2003.2), Russian Ministry for Industry and Science (Project on Superconductivity of Mesoscopic and Strongly Correlated Systems), and the Natural Sciences and Engineering Research Council of Canada (NSERC) is gratefully acknowledged. A Moewes is a Canada Research Chair. The work at the Advanced Light Source at Lawrence Berkeley National Laboratory was supported by the US Department of Energy (Contract DE-AC03-76SF00098).

References

[1] Nagamatsu J, Nakagawa N, Muronaka T, Zenitani Y and Akimitsu J 2001 *Nature* **410** 63
[2] Burdett J K and Miller C J 1989 *Chem. Mater.* **2** 12
[3] Wörle M, Nesper R, Mair G, Schwarz M and Schnering H G 1995 *Z. Anorg. Allg. Chem.* **621** 1153
[4] An J M and Pickett W E 2001 *Phys. Rev. Lett.* **86** 4366
[5] Rosner H, Kitaigorodsky A and Pickett W E 2002 *Phys. Rev. Lett.* **88** 127001
[6] Ravindran P, Vajeeston P, Vidya R, Kjekshus A and Fjellvag H 2001 *Phys. Rev.* B **64** 224509
[7] Dewhurst J K, Sharma S, Ambrosch-Drax C and Johansson B 2003 *Phys. Rev.* B **68** 20504
[8] Kobayashi K and Arai M 2002 *J. Phys. Soc. Japan* **71** 217
[9] Bharathi A, Jemima Balaselvi S, Premila M, Sairam T N, Reffy G L N, Sunder C S and Hariharan Y 2002 *Solid State Commun.* **124** 423
[10] Fogg A M, Claridge J B, Darling G R and Rosseinsky M J 2003 *Preprint* cond-mat/0304662
[11] Methfessel M, van Schilfgaarde M and Casali R A 2000 *Electronic Structure and Physical Properties of Solids: The Uses of the LMTO Method* (*Springer Lecture Notes in Physics* vol 535) ed H Dreysse (Berlin: Springer)
[12] Lüning J, Rubensson J-E, Ellmers G, Eisebitt S and Eberhardt W 1997 *Phys. Rev.* **56** 13147
[13] Ma Y, Wassdahl N, Skytt P, Guo J, Nordgren J, Johnson P D, Rubensson J-E, Boske T, Eberhardt W and Kevan S D 1992 *Phys. Rev. Lett.* **69** 2598